Characterization of the 2-(α-Carbolinyl)nitrenium Ion and Its Conjugate Base Produced during the Decomposition of the Model Carcinogen 2-*N*-(Pivaloyloxy)-2-amino-α-carboline in Aqueous Solution

Michael Novak* and Shahrokh Kazerani

Contribution from the Department of Chemistry and Biochemistry, Miami University, Oxford, Ohio 45056

Received September 21, 1999. Revised Manuscript Received December 16, 1999

Abstract: The kinetics of the decomposition of the model ultimate carcinogen 2-*N*-(pivaloyloxy)-2-amino-α-carboline (**4a**), and its 9-methyl analogue (**4b**), in 20 vol % CH_3CN-H_2O, $\mu = 0.5$ ($NaClO_4$) at 20 °C, are consistent with the uncatalyzed N−O bond heterolysis of the neutral esters. The protonated ester **4aH**$^+$ ($pK_a = 1.6$), detected kinetically and by spectrophotometric titration, is unreactive under these conditions. Spectrophotometric titration of **4b** also indicates that a protonated species, **4bH**$^+$ ($pK_a = 0.9$), is formed under acidic conditions. Both **4a** and **4b** produce electrophilic intermediates, identified as the nitrenium ions **5a** and **5b**, that are efficiently trapped by N_3^-, Br^-, and 2′-deoxyguanosine, d-G, without an increase in the overall rate of decomposition of the esters. N_3^- and d-G trapping efficiencies, k_{az}^+/k_s^+ and k_{d-G}^+/k_s^+, for **5a** and **5b** are very similar to each other and are within a factor of 4 of the trapping efficiencies with N_3^- and d-G previously measured for the 2-fluorenylnitrenium ion (**6**). The trapping efficiencies for **5a**, but not **5b**, decrease with increasing pH. These results indicate that **5a** is deprotonated at the indolyl nitrogen to produce a neutral intermediate (**7a**) that retains reduced reactivity with Br^-, N_3^-, and d-G in an aqueous environment. The neutral **7a** undergoes reduction and dimerization reactions in the absence of nonsolvent nucleophiles much more efficiently than its conjugate acid. Microscopic rate constants for trapping of **5a** and **7a** by the three nucleophiles and the pK_a for ionization of **5a** to produce **7a** have been estimated from experimental data, from the assumption of diffusion control of the reaction of **5a** with N_3^-, and by analogy to the reactions of structurally related species. The relatively low mutagenicity and carcinogenicity of the parent amine, 2-amino-α-carboline (**3a**), may be related to the fact that the less selective neutral species **7a** is responsible for the reaction with nucleophiles at neutral pH.

Heterocyclic arylamines are ubiquitous mutagens and carcinogens found in parts per billion concentrations in broiled and fried meats and other protein-containing foods, as well as in tobacco smoke.[1] These materials are pyrolysis products of proteins and amino acids,[2] and are not direct acting mutagens toward *Salmonella.*[3] Similar to their carbocyclic analogues, these materials require oxidative metabolism, usually provided by mammalian liver homogenates, to exhibit mutagenicity toward *Salmonella* in Ames tests.[3]

The overall metabolic pathway that generates the ultimate mutagens/carcinogens, sulfuric or carboxylic acid esters of the hydroxylamine derivatives of the amines, is outlined in Scheme 1.[3,4] On the basis of the similarities of the metabolism and DNA adducts derived from heterocyclic and carbocyclic arylamines, it is widely assumed that the ester metabolites of heterocyclic arylamines undergo heterolytic N−O bond cleavage to generate nitrenium ions that are responsible for the mutagenic and carcinogenic effects of these materials.[1,5] It is now firmly established that the highly mutagenic and carcinogenic esters of carbocyclic arylamines do generate selective nitrenium ions in aqueous media that are responsible for the formation of DNA adducts.[6,7] A recent report also showed that appropriate ester derivatives, **1a**−**c**, of the weakly mutagenic 2-amino-5-phenylpyridine (Phe-P-1), and related amines, generate electrophilic

* To whom correspondence should be addressed. Phone: (513) 529-2813. Fax: (513) 529-5715. E-mail: novakm@muohio.edu.

(1) Eisenbrand, G.; Tang, W. *Toxicology* **1993**, *84*, 1−82. Hatch, F. T.; Knize, M. G.; Felton, J. S. *Environ. Mol. Mutagen.* **1991**, *17*, 4−19. Layton, D. W.; Bogen, K. T.; Knize, M. G.; Hatch, F. T.; Johnson, V. M.; Felton, J. S. *Carcinogenesis* **1995**, *16*, 39−52. Sugimura, T. *Environ. Health Perspect.* **1986**, *67*, 5−10.

(2) Kasai, H.; Yamaizumi, Z.; Wakabayashi, K.; Nagao, M.; Sugimura, T.; Yokoyama, S.; Miyazawa, T.; Nishimura, S. *Chem. Lett.* **1980**, 1391−1394. Jagerstad, M.; Gisson, K.; Grivas, S.; Negishi, C.; Wakabayashi, K.; Tsuda, M.; Sato, S.; Sugimura, T. *Mutat. Res.* **1984**, *126*, 239−244. Yoshida, D.; Matsumoto, T.; Yoshimura, R.; Matsuzaki, T. *Biochem. Biophys. Res. Commun.* **1978**, *83*, 915−920. Yoshida, D.; Matsumoto, T.; Okamoto, H.; Mizusaki, S.; Kushi, A.; Fukuhara, U. *Environ. Health Perspect.* **1986**, *67*, 55−58.

(3) Sugimura, T. *Mutat. Res.* **1985**, *150*, 33−41. Felton, J. S.; Knize, M. G.; Shen, N. H.; Andersen, B. D.; Bjeldanes, L. F.; Hatch, F. T. *Environ. Health Perspect.* **1986**, *67*, 17−24.

(4) Shinohara, A.; Saito, K.; Yamazoe, Y.; Kamataki, T.; Kato, R. *Cancer Res.* **1986**, *46*, 4362−4367. Aoyama, T.; Gonzalez, F. J.; Gelboin, H. V. *Mol. Carcinogen.* **1989**, *2*, 192−198. Snyderwine, E. G.; Wirth, P. J.; Roller, P. P.; Adamson, R. H.; Sato, S.; Thorgiersson, S. S. *Carcinogenesis* **1988**, *9*, 411−418. Meerman, J. H. N.; Ringer, D. P.; Coughtrie, M. W. H.; Bamforth, K. J.; Gilissen, R. A. H. J. *Chem.-Biol. Interact.* **1994**, *92*, 321−328. Raza, H.; King, R. S.; Squires, R. B.; Guengerich, F. P.; Miller, D. W.; Freeman, J. P.; Lang, N. P.; Kadlubar, F. F. *Drug Metab. Dispos.* **1996**, *24*, 385−400. Watanabe, M.; Ishidate, M.; Nobmi, T. *Mutat. Res.* **1990**, *234*, 337−348.

(5) Saris, C. P.; van Dijk, W. J.; Westra, J. G.; Hamzink, M. R. J.; van de Werken, G.; Zomer, G.; Stavenuiter, J. F. C. *Chem.-Biol. Interact.* **1995**, *95*, 29−40. Hashimoto, Y.; Shudo, K.; Okamoto, T. *Biochem. Biophys. Res. Commun.* **1980**, *96*, 355−362. Snyderwine, E. G.; Roller, P. P.; Adamson, R. H.; Sato, S.; Thorgiersson, S. S. *Carcinogenesis* **1988**, *9*, 1061−1065.

10.1021/ja993433e CCC: $19.00 © 2000 American Chemical Society
Published on Web 03/24/2000

Scheme 1

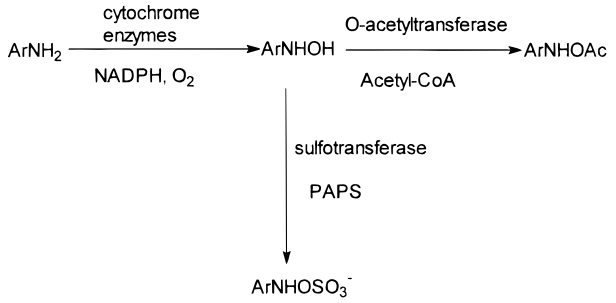

intermediates, identified as nitrenium ions **2a**−**c**, that are trapped by N_3^-, although far less efficiently than the 4-biphenylylnitrenium ion, **2d**, that is generated from **1d**.[8]

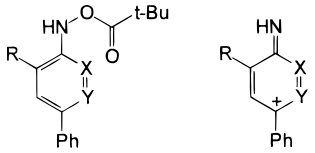

a X = N, Y = CH, R = H
b X = N, Y = CH, R = CH_3
c X = CH, Y = N, R = H
d X = CH, Y = CH, R = H

Phe-P-l is not highly representative of the class of mutagenic and carcinogenic heterocyclic arylamines in that it is isolated in lower concentrations than other heterocyclic amines in cooked meats, and is very weakly mutagenic compared to other members of the class.[1,3] The amine 2-amino-α-carboline (AαC, **3a**) is among the more prevalent carcinogenic and mutagenic

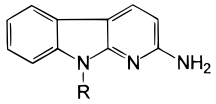

3

a R = H
b R = CH_3

heterocyclic arylamines found in cooked meats.[1] It also shows mutagenicity toward *Salmonella* that is quantitatively similar to that of the well-known carbocyclic carcinogenic amine 2-aminofluorene, although it is a relatively weak mutagen and carcinogen in comparison to other members of the class of heterocyclic arylamines.[1,3] Ester derivatives of **3a** were chosen as one of the targets for our continuing study of the chemical basis of arylamine carcinogenesis because of the relative abundance of this amine in cooked meats and because of potentially unique features of the chemistry of these esters.

Scheme 2

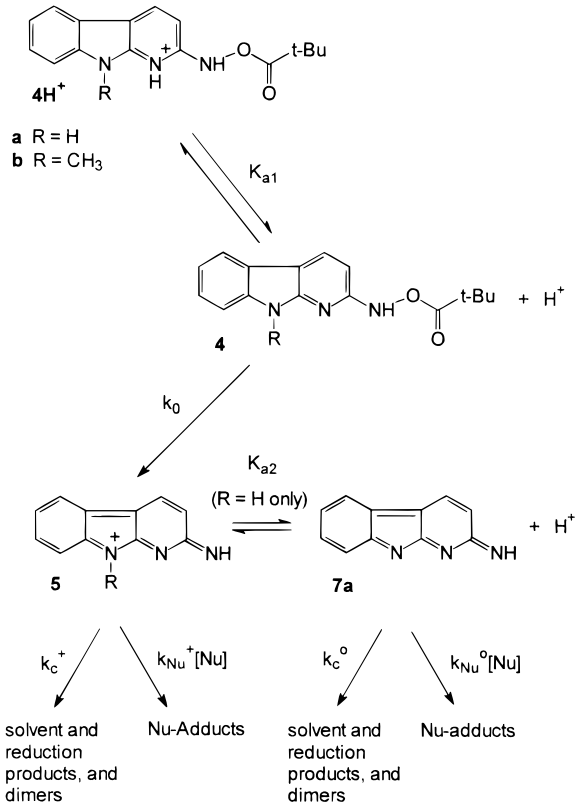

The model ester derivative of **3a**, 2-*N*-(pivaloyloxy)-2-amino-α-carboline, **4a**, was synthesized to examine the reactivity and selectivity of its potential N−O bond heterolysis product, the 2-(α-carbolinyl)nitrenium ion, **5a** (Scheme 2), an aza analogue to the well studied 2-fluorenylnitrenium ion, **6**.[6d,7c,d] The ion

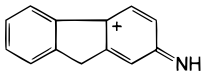

6

5a also has the potential to undergo deprotonation to form the quinone imine methide, **7a** (Scheme 2). This deprotonation could be biologically relevant because **7a** is unlikely to have chemical properties identical to those of **5a**. This potential deprotonation could also be a feature of nitrenium ions derived from several other carcinogenic and mutagenic heterocyclic arylamines, including Trp-P-1 and Trp-P-2 (**8a** and **8b**).

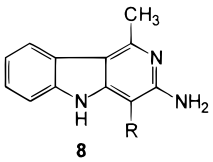

8

a R = CH_3
b R = H

In this paper we report our studies that show that **4a** and its 9-methyl analogue **4b** do generate reactive electrophiles, identified as **5a** and **5b**, respectively, that are efficiently trapped by Br^-, N_3^-, and 2′-deoxyguanosine, d-G. The rate constant ratios for competitive trapping of **5a** and **5b** by N_3^- and solvent (k_{az}^+/k_s^+) and d-G and solvent (k_{d-G}^+/k_s^+) are within an order of magnitude of those previously reported for **6**.[6d,7c,d]

(6) (a) Novak, M.; Kahley, M. J.; Eiger, E.; Helmick, J. S.; Peters, H. E. *J. Am. Chem. Soc.* **1993**, *115*, 9453−9460. (b) Davidse, P. A.; Kahley, M. J.; McClelland, R. A.; Novak, M. *J. Am. Chem. Soc.* **1994**, *116*, 4513−4514. (c) Novak, M.; Kahley, M. J.; Lin, J.; Kennedy, S. A.; Swanegan, L. A. *J. Am. Chem. Soc.* **1994**, *116*, 11626−11627. (d) McClelland, R. A.; Davidse, P. A.; Hadzialic, G. *J. Am. Chem. Soc.* **1995**, *117*, 4173−4174.

(7) (a) Novak, M.; Kennedy, S. A. *J. Am. Chem. Soc.* **1995**, *117*, 574−575. (b) Kennedy, S. A.; Novak, M.; Kolb, B. A. *J. Am. Chem. Soc.* **1997**, *119*, 9, 7654−7664. (c) McClelland, R. A.; Gadosy, T. A.; Ren, D. *Can. J. Chem.* **1998**, *76*, 1327−1337. (d) McClelland, R. A.; Abmad, A.; Dicks, A. P.; Licence, V. E. *J. Am. Chem. Soc.* **1999**, *121*, 3303−3310.

(8) Novak, M.; Xu, L.; Wolf, R. A. *J. Am. Chem. Soc.* **1998**, *120*, 1643−1644.

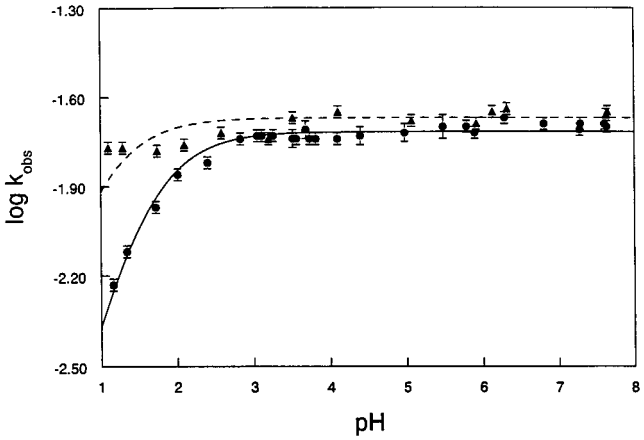

Figure 1. log k_{obs} vs pH for **4a** (●) and **4b** (▲). The theoretical line for **4a** (solid) was obtained from a least-squares fit of the rate constants to eq 1. The theoretical line for **4b** (dashed) was obtained in a similar manner with the pK_a of 0.89 ± 0.23 obtained from spectrophotometric titration.

Trapping of **5b** by N_3^-, Br^-, and d-G is pH independent in the pH range 3−8, but the trapping of **5a** by these nucleophiles is pH dependent in a manner consistent with the proposed deprotonation of Scheme 2. Since the deprotonated species **7a** is much less selective toward these nucleophiles, in part, because of a facile reduction reaction, and it predominates under neutral pH conditions, the relatively low mutagenicity and carcinogenicity of **3a** compared to other heterocyclic arylamines may be related to this ionization equilibrium.

Results

The rates of decomposition of **4a** and **4b** at initial concentrations of ca. 1.0×10^{-5} M were monitored by UV methods at 20 °C in 20 vol % CH_3CN-H_2O at $\mu = 0.5$ ($NaClO_4$) in the pH range 1−8 in tris/trisH^+, Na_2HPO_4/NaH_2PO_4, NaOAc/HOAc, and HCO_2Na/HCO_2H buffers at pH > 2.5, and in $HClO_4$ solutions at pH ≤ 2.5. Absorbance vs time measurements cleanly followed the first-order rate equation for at least 5 half-lives for **4b** at all pH values and for **4a** at pH < 5. At pH > 5 the kinetics of the decomposition of **4a** were complicated by the precipitation of one of the reaction products (vide infra), but the decomposition of **4a** still appeared to be first-order in nature if data were taken for ca. 4 half-lives. Rate constants were buffer independent, but exhibited pH dependence for **4a** in this pH range. The pH dependence of k_{obs} for **4a** and **4b** is summarized in Figure 1, and a table of rate constants collected under all pH conditions for both esters is presented in the Supporting Information.

The pH dependence of k_{obs} for **4a** was adequately fit by eq 1. The pH dependence of the initial UV absorbance of **4a** at 360 nm (Figure 2) is also consistent with an ionization

$$k_{obs} = k_o K_{a1}/(K_{a1} + 10^{-pH}) \quad (1)$$

equilibrium. The pK_a values derived from the kinetic fit and from the initial absorbance data are in good agreement (Table 1). In this pH range the decomposition of **4b** did not exhibit significant pH dependence, but a plot of initial absorbance for **4b** at 360 nm vs H_o[9] or pH in the range −1.0 to +2.5 (Figure 2) could be fit to a titration curve to obtain a pK_{a1} of 0.89 ± 0.23. The kinetic data for **4b** were also fit to eq 1 with the K_{a1} obtained from the UV absorbance data. The kinetic fits obtained for **4a** and **4b** are summarized in Table 1. Rate data for **4a** in 5 vol % CH_3CN-H_2O are included for comparison to those for **1a**.[8]

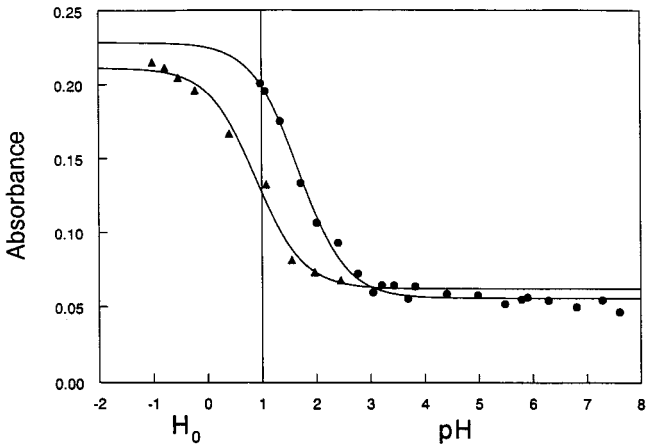

Figure 2. Initial absorbance at 360 nm vs pH or H_o for **4a** (●) and **4b** (▲). Theoretical lines were obtained from a fit of the data to a standard titration equation.

Table 1. Summary of Kinetic Data for **4a** and **4b**[a]

		pK_{a1}		
ester	conditions	kinetic fit	UV absorbance	k_o (s^{-1})
4a	5% CH_3CN	1.73 ± 0.06		$(8.3 \pm 0.2) \times 10^{-2}$
4a	20% CH_3CN	1.55 ± 0.05	1.68 ± 0.12	$(1.92 \pm 0.02) \times 10^{-2}$
4b	20% CH_3CN		0.89 ± 0.23	$(2.14 \pm 0.06) \times 10^{-2}$
1a[b]	5% CH_3CN	2.5 ± 0.3	2.83 ± 0.05	$(6.7 \pm 0.4) \times 10^{-6}$

[a] Determined at 20 °C and $\mu = 0.5$ ($NaClO_4$). [b] From ref 8.

The pH dependence of k_{obs} for **1a**−**c** also followed eq 1.[8] Since the rate constants for decomposition of the carbocyclic ester **1d** showed no such pH dependence, the ionization equilibrium for **1a**−**c** was attributed to protonation of the pyridyl nitrogen of these esters.[8] The same interpretation is assumed for **4a**. Equation 1 implies that **4aH**$^+$ is hydrolytically unreactive and **4a** undergoes a pH- and buffer-independent decomposition (Scheme 2). Data in Table 1 show that the limiting decomposition rate constant for **4a**, k_o, is ca. 10^4 larger than k_o for **1a** under the same conditions. The pK_a data indicate that **4aH**$^+$ is a ca. 10-fold stronger acid than **1aH**$^+$. This is consistent with the expected inductive effect of the indole nitrogen of **4aH**$^+$.

Although it was not possible to confirm the existence of a similar ionization equilibrium for **4b** from the kinetic data because rate measurements were not made below pH 1, the spectrophotometric titration of **4b** indicates that a protonation of this compound also occurs under acidic conditions. Since the spectral changes associated with protonation of **4a** and **4b** are very similar, it is likely that the pK_a refers to ionization of **4bH**$^+$. The ΔpK_a of ca. 0.8 for **4aH**$^+$−**4bH**$^+$ is at first glance surprising. Apparently the 9-methyl substituent of **4bH**$^+$ is situated so that, in combination with the pivaloyloxy substituent, it can effectively limit solvation of the cation by solvent, and therefore increase the acidity of **4bH**$^+$ relative to **4aH**$^+$. Similar effects have previously been observed for **9aH**$^+$ and **9bH**$^+$ in

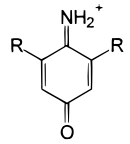

9H$^+$

a R = H
b R = CH_3

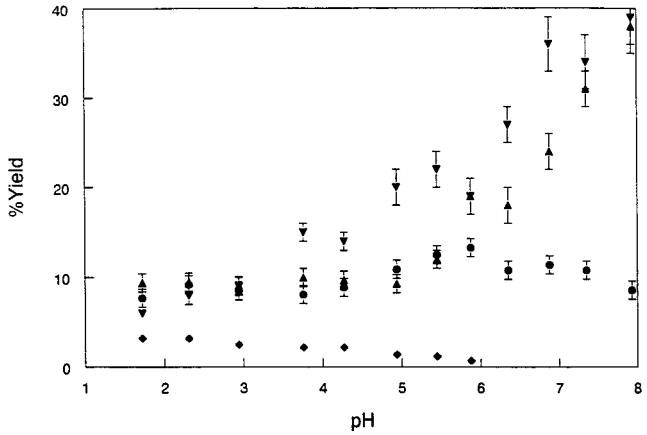

Figure 3. Product yields vs pH for **4a**: **3a** (●), **10a** (▲), **10b** (▼), **11** (◆). The dimer **10c** is produced in low yields (<5%) at all pH values.

which ΔpK_a is 0.7 and for the 2,6-diisopropylpyridinium ion and 2,6-di-*tert*-butylpyridinium ion in which ΔpK_a is 1.8.[10,11] Although the 9-methyl substituent of **4b** has a significant effect on pK_{a1}, it has a negligible effect on k_o (Table 1). The ratio of k_o values determined for **4b**/**4a** is 1.11 ± 0.03, so the 9-methyl substituent accelerates the decomposition of **4b**, but only by a factor of ca. 10% over **4a**.

The products of the decomposition of **4a** were examined over the pH range of the kinetic studies. The results are summarized in Figure 3. Under neutral pH conditions the products consist predominantly of the amine **3a** and three dimeric products, **10a**−**c**, that appear to be derived from reaction of **3a** with the

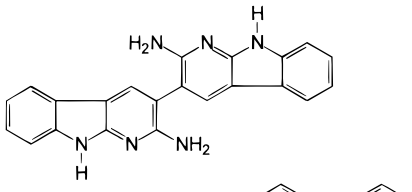

10a

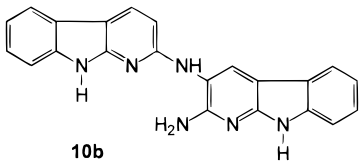

10b

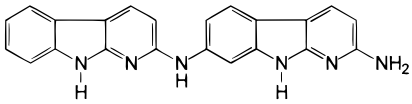

10c

nitrenium ion **5a** or its conjugate base **7a**. Since the decomposition of **4a** remains first-order throughout the pH range of the study, these dimers must be produced after the rate-limiting step of the decomposition of **4a**. One of the dimers, **10b**, slowly precipitates from solution at neutral pH, but it remains in solution long enough for HPLC analysis of reaction products as long as the analysis is initiated within ca. 5 half-lives of the decomposition of **4a** (ca. 3 min at pH > 2.5). Under neutral pH conditions these four products account for most of **4a**. For example, at pH 7.35 the combined yields of **3a** (11 ± 1%), **10a** (31 ± 2%), **10b** (34 ± 3%), and **10c** (4 ± 1%) account for 80

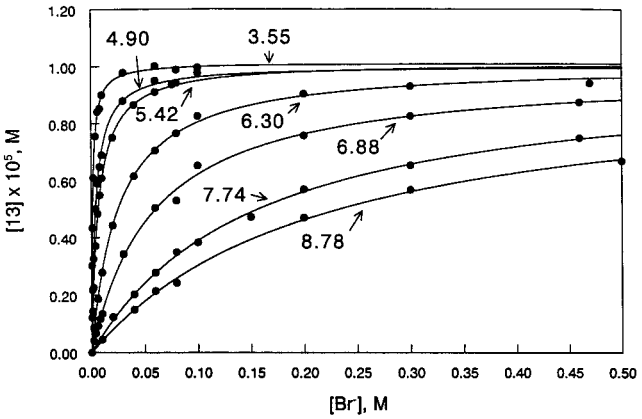

Figure 4. Br^- adduct concentration [**13**] vs [Br^-] at the indicated pH. Theoretical lines at each pH were calculated from a least-squares fit to eq 2. Initial concentration of **4a** was 1.0×10^{-5} M.

± 4% of the initial **4a** (yields of the dimers are reported to take into account the fact that 1 mol of dimer is produced by 2 mol of **4a**). At lower pH the yields of the dimers drop off dramatically, while the yield of **3a** remains roughly constant (Figure 3). For example, at pH 2.94 a yield of 8.5 ± 1.0% of **3a** is observed, while the combined yield of **10a**−**c** is reduced to 18 ± 2%. Although the yields of the dimers decrease significantly at lower pH, no major stable product that replaces them could be found. One minor product, **11**, appears to be

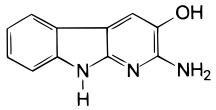

11

formed at the expense of the dimers since it cannot be observed at neutral pH, but reaches a constant yield of 3.0 ± 0.2% below pH 4. On the basis of analogy to the reactions of **6** and other carbocyclic nitrenium ions, the expected major initial product of attack of solvent on **5a** would be **12**.[6] Neither this product

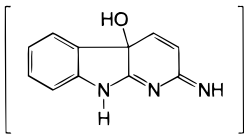

12

nor any of its expected decomposition products were detected at any pH. The observed yields of the known products **3a**, **10a**−**c**, and **11** account for only ca. 30% of **4a** at pH < 4, so there must be a major product(s) formed under acidic pH conditions that we have not been able to isolate.

Although the yield of products formed from the decomposition of **4a** in the absence of trapping agents is far from quantitative under acidic pH conditions, trapping by Br^- or N_3^- does produce quantitative yields of products over the entire pH range at sufficiently high concentrations of the trapping agent. This is illustrated in Figure 4 for trapping by Br^-. The yield of the Br^- adduct **13** measured as a function of [Br^-] was fit to eq 2 to produce the theoretical lines shown in Figure 4 (see Scheme 2 for definitions of k_c and k_{Nu}).[12]

(9) Paul, M. A.; Long, F. A. *Chem. Rev.* **1957**, *57*, 1−45.
(10) Novak, M.; Martin, K. A. *J. Org. Chem.* **1991**, *56*, 1585−1590.
(11) Condon, F. E. *J. Am. Chem. Soc.* **1965**, *87*, 4494−4496. Brown, H. C.; Kanner, B. *J. Am. Chem. Soc.* **1966**, *88*, 986−992.
(12) Fishbein, J. C.; McClelland, R. A. *J. Am. Chem. Soc.* **1987**, *109*, 2824−2825. The derivation of this equation assumes that k_s is a pseudo-first-order rate constant. This is unlikely, at least at neutral pH, because of the detection of **10a**−**c**. Nevertheless, the data fit the equation very well.

$$[\text{adduct}] = \frac{(k_{Nu}/k_c)_{obs}[\text{adduct}]_{max}[Nu]}{1 + (k_{Nu}/k_c)_{obs}[Nu]} \quad (2)$$

The saturation yield of **13** obtained from the fit, $[\mathbf{13}]_{max}$, averaged 100 ± 4% of the initial concentration of **4a** at all pH values examined. Figure 4 shows that the trapping efficiency of Br^-, $(k_{Br}/k_c)_{obs}$, is pH dependent. $\log(k_{Br}/k_c)_{obs}$ vs pH data (Figure 5) were fit to a standard titration curve to obtain the limiting trapping efficiencies under acidic and neutral pH conditions, k_{Br}^+/k_c^+ and k_{Br}^0/k_c^0, respectively (Table 3). An apparent pK_a, pK_{a2}^{app}, of 4.7 ± 0.4 was also obtained from the fit. Rate constant data shown in Table 2 indicate that Br^- does not accelerate the rate of disappearance of **4a**, although it has a major effect on product distributions.

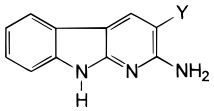

13 Y = Br
14 Y = N_3

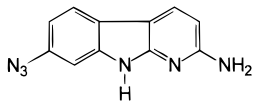

15

Trapping by N_3^- showed similar behavior except that N_3^- is a more efficient trap than Br^-. The combined saturation yields of the two N_3^- adducts **14** and **15**, obtained from fits of [**14**] and [**15**] vs $[N_3^-]$ to eq 2, accounted for 99 ± 12% of the initial concentration of **4a** over the pH range of the study. In these studies $[N_3^-]$ was calculated from the total azide added as NaN_3, the measured pH of the solutions, and the apparent pK_a of HN_3 measured in this solvent (4.59). The trapping efficiencies, $(k_{az}/k_c)_{obs}$, obtained from the fits to eq 2 for both **14** and **15** were in good agreement (±25%), and a plot of the average value of $\log(k_{az}/k_c)_{obs}$ vs pH (Figure 6) shows that trapping is pH dependent. A fit to a standard titration curve produced the theoretical line shown in Figure 6. The apparent pK_a of 5.1 ± 0.2 is experimentally indistinguishable from pK_{a2}^{app} measured from Br^- trapping.

The ratio of the calculated saturation yields of **14** and **15**, $[\mathbf{14}]_{max}/[\mathbf{15}]_{max}$, is also pH dependent (Figure 7). A fit of these data to a standard titration curve produces an apparent pK_a, pK_{a3}^{app}, of 6.5 ± 0.2 that is clearly different from pK_{a2}^{app}. Figure 7 shows that $[\mathbf{14}]_{max}/[\mathbf{15}]_{max}$ increases from 2.0 ± 0.1 under acidic conditions to 3.9 ± 0.2 under neutral pH conditions. The data in Table 2 show that N_3^- does not increase the rate of decomposition of **4a** under conditions in which the two N_3^- adducts **14** and **15** account for more than 90% of the reaction products of **4a**.

Less extensive trapping studies of the reaction of **4a** with d-G were also performed. The structure of the isolated reaction product, **16**, was deduced from spectral data and confirmed by its acid-catalyzed conversion into the previously characterized guanine adduct **17**.[13] The yield of **16**, measured as a function

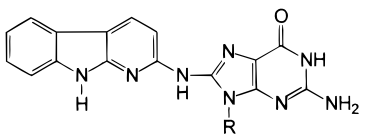

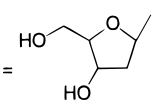

16 R =

17 R = H

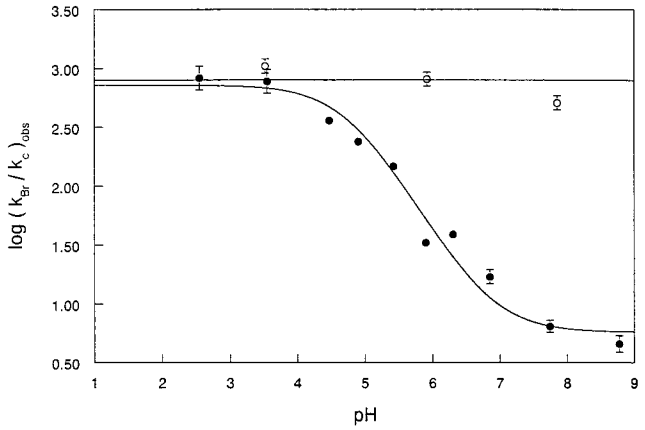

Figure 5. $\log(k_{Br}/k_c)_{obs}$ vs pH for **4a** (●) and **4b** (▲). The theoretical line for **4a** was obtained from a least-squares fit to a standard titration curve. The theoretical line for **4b** is the average of the observed values.

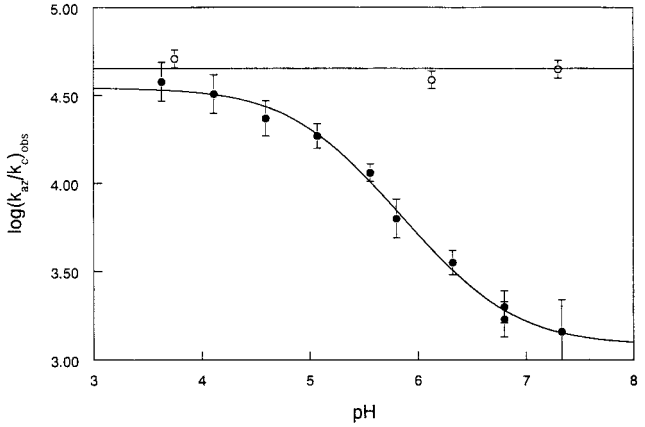

Figure 6. $\log(k_{az}/k_c)_{obs}$ vs pH for **4a** (●) and **4b** (▲). The theoretical lines for **4a** and **4b** were calculated as described in Figure 5.

of [d-G] at pH 7.28 and 4.10, fit eq 2 well, and trapping was pH dependent. Measurements of the rate constant for disappearance of **4a** in the presence of d-G (Table 2) showed that d-G does not accelerate the rate of decomposition of **4a**.

The pH-dependent trapping results for all three nucleophiles are summarized in Table 3. The selectivity data from which these results were obtained are reported in the Supporting Information. The results show that N_3^- is the most efficient trap of the three nucleophiles under both acidic and neutral pH conditions. For both N_3^- and d-G the trapping efficiency under acidic conditions is ca. 30-fold greater than under neutral conditions, while for Br^- the trapping efficiency under acidic conditions is ca. 120-fold greater than under neutral conditions.

One of the decomposition products of **4b** was identified by HPLC co-injection as the amine **3b**. This is analogous to the observation of **3a** as one of the decomposition products of **4a**. Like **3a**, **3b** was detected at a low, pH-independent, yield of 9 ± 1% in the pH range 3.5−8.0. Low yields of two apparently dimeric products with HPLC retention times similar to those of **10a**−**c** were also detected. Unlike **10a**−**c**, the yields of these products did not change significantly with pH. If the extinction coefficients for these products are in the same range as those for **10a**−**c**, the combined yields of these two materials is less than 15% throughout the pH range. No other significant products were detected by HPLC in the absence of nucleophilic trapping agents.

(13) Pfau, W.; Schulze, C.; Shirai, T.; Hasegawa, R.; Brockstedt, U. *Chem. Res. Toxicol.* **1997**, *10*, 1192−1197.

Table 2. Comparison of k_{obs} for **4a** and **4b** in the Presence and Absence of N_3^-, Br^-, or d-G[a]

	$k_{obs} \times 10^2$ (s^{-1})			
	no added nucleophile	NaN_3 added, $[N_3^-]$ (M) (% trapping)[b]	NaBr added, $[Br^-]$ (M) (% trapping)[b]	d-G added, [d-G] (M) (% trapping)[b]
		For **4a**		
7.64	2.01 ± 0.04	1.65 ± 0.04 [0.02] (96)	1.73 ± 0.04 [0.45] (75)	
7.28	1.93 ± 0.04			1.79 ± 0.04 [0.03] (88)
4.10	1.83 ± 0.04			1.80 ± 0.04 [0.003] (96)
3.74	1.81 ± 0.04	1.65 ± 0.04 [0.002] (99)		
3.52	1.84 ± 0.05		2.00 ± 0.04 [0.06] (98)	
		For **4b**		
4.11	2.23 ± 0.03	1.73 ± 0.03 [0.001] (98)		2.17 ± 0.08 [0.002] (95)
3.52	2.16 ± 0.03		1.79 ± 0.04 [0.01] (89)	

[a] Measured in 20 vol % CH_3CN-H_2O in 0.02 M buffers maintained with Na_2HPO_4/NaH_2PO_4 or NaOAc/HOAc, at 20 °C and $\mu = 0.5$ ($NaClO_4$). [b] For **4a**, calculated from eq 2 at the indicated concentration of the nucleophile using $(k_{Nuc}/k_c)_{obs}$ taken from the theoretical lines in Figures 5 and 6 for Br^- and N_3^-, respectively, and from the directly measured $(k_{d-G}/k_c)_{obs}$ for d-G. For **4b**, calculated from eq 2 at the indicated concentration of nucleophile using the average $(k_{Nu}/k_c)_{obs}$ for the nucleophile.

Table 3. Summary of Trapping Data for **4a** and **4b** in the Presence of Br^-, N_3^-, and d-G

For **4a**

nucleophile	k_{Nu}^+/k_c^+ (M^{-1})[a]	k_{Nu}^0/k_c^0 (M^{-1})[a]	pK_{a2}^{app} [a]	pK_{a3}^{app} [b]
N_3^-	$(3.5 \pm 0.3) \times 10^4$	$(1.2 \pm 0.1) \times 10^3$	5.1 ± 0.2	6.5 ± 0.2
Br^-	$(7.2 \pm 1.6) \times 10^2$	5.8 ± 1.4	4.7 ± 0.4	
d-G	$(8.2 \pm 0.6) \times 10^3$[c]	$(2.4 \pm 0.1) \times 10^2$[d]		

For **4b**

nucleophile	$(k_{Nu}/k_c)_{obs}$ (M^{-1})[e]
N_3^-	$(4.5 \pm 0.6) \times 10^4$
Br^-	$(8.0 \pm 2.7) \times 10^2$
d-G	$(8.8 \pm 0.5) \times 10^3$

[a] From fits of $(k_{Nu}/k_c)_{obs}$ vs pH to a standard titration curve unless otherwise indicated. [b] From a fit of $[\mathbf{14}]_{max}/[\mathbf{15}]_{max}$ vs pH to a standard titration curve. [c] $(k_{d-G}/k_c)_{obs}$ at pH 4.10. [d] $(k_{d-G}/k_c)_{obs}$ at pH 7.28. [e] The average value observed over the entire pH range.

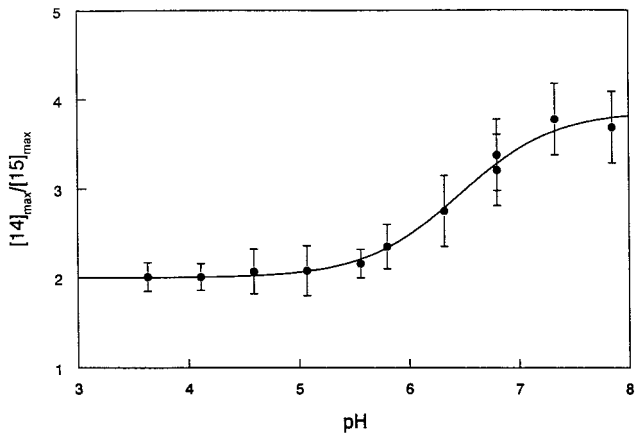

Figure 7. Azide adduct product ratio $[\mathbf{14}]_{max}/[\mathbf{15}]_{max}$ vs pH. The data were fit to a standard titration curve.

Products of the trapping of the decomposition of **4b** with the three nucleophiles were monitored by HPLC. In all three cases products with HPLC retention times similar to those of the corresponding adducts of **4a** were observed. These products were not isolated, but their HPLC peak areas varied with [Nu] in a manner consistent with eq 2. The values of $(k_{Nu}/k_c)_{obs}$ obtained from these fits did not vary with pH in the pH range in which the $(k_{Nu}/k_c)_{obs}$ data for **4a** showed considerable pH dependence (Figures 5 and 6 and Table 3). Average values for $(k_{Nu}/k_c)_{obs}$ for Br^-, N_3^-, and d-G for **4b** are gathered in Table 3, and individual results of trapping experiments are reported in the Supporting Information. For all three nucleophiles $(k_{Nu}/k_c)_{obs}$ is comparable to k_{Nu}^+/k_c^+ of **4a** for the corresponding nucleophile. The trapping efficiency of N_3^- is ca. 30% higher for **4b** than for **4a** under acidic conditions. For the other two nucleophiles, the trapping efficiencies for **4a** and **4b** are experimentally indistinguishable. Rate constant data in Table 2 confirm that the trapping occurs without acceleration of the decomposition of **4b**.

Some preliminary attempts were made to investigate the source of the reduction product **3a** derived from the decomposition of **4a**. Falvey and co-workers have previously shown that Ph_3CH can efficiently trap triplet nitrenium ions to generate the corresponding amine and the radical coupling product **18**.[14]

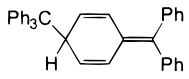

18

Decomposition of 1×10^{-5} M **4a** in N_2 outgassed pH 6.7 phosphate buffer saturated with Ph_3CH (2.8×10^{-5} M) led to a slight increase in the yield of **3a** from 7 ± 1% in the absence of Ph_3CH to 10 ± 1% in its presence. The dimer **18** was not detected, but an HPLC peak consistent with a low yield of Ph_3COH was detected. Decomposition of 1×10^{-5} M **3a** in the presence of leucomalachite green, **19**, saturated at 4.0×10^{-5} M in pH 7.3 phosphate buffer led to a much larger effect on reaction products. In the presence of **19** the yield of **3a**

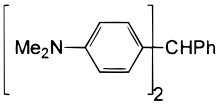

19

(14) Srivastava, S.; Falvey, D. E. *J. Am. Chem. Soc.* **1995**, *117*, 10186−10193.

increased to 37 ± 2% from the observed yield of 14 ± 1% in the control experiment run in the absence of any traps. The yields of the dimers **10a** and **10b** were also strongly affected by the presence of **19**. The yield of **10a** decreased from 28 ± 2% in the absence of **19** to 9.6 ± 0.4% in its presence, while **10b** showed a similar decrease in yield from 31 ± 2% to 10 ± 1%.

Discussion

Most of the characteristics of the decomposition of **4a** are similar to those previously observed for analogous carbocyclic and heterocyclic esters that generate nitrenium ions.[6−8] The pH dependence of the kinetics of the decomposition of **4a** is similar to that previously observed for **1a**−**c**, and is consistent with rate-limiting uncatalyzed N−O bond cleavage of the neutral ester.[8] The conjugate acid, **4aH**$^+$, is unreactive in the pH range of this study. N_3^-, Br^-, and d-G act as efficient nucleophilic traps to generate products the structures of which are consistent with trapping of a nitrenium ion. The structure of the C-8 adduct **16** is, in particular, characteristic of the products of nitrenium ion trapping by d-G.[7] The lack of a rate acceleration for ester decomposition at high trapping efficiencies by N_3^-, Br^-, and d-G (Table 2) is classical evidence for a $D_N + A_N$ (S_N1) mechanism with rate-limiting ionization.[6,7,15,16] The data in Table 2 show moderate (5−15%) decreases in k_{obs} in the presence of some of the trapping agents. The origin of this apparent deceleration is not clear. Since it can occur at very low concentrations of the added nucleophile, it is unlikely to be a specific salt effect. The common feature of all the rate data obtained in the presence of the nucleophiles is that they were gathered under conditions of high trapping efficiency in which the yields of the dimeric products **10a**−**c** are minimal. At least one of these products (**10b**) is known to precipitate from solution during the reaction. This process, or other potentially slow processes associated with the formation of the dimers, may cause an apparent small increase in k_{obs} without significantly affecting the fit of the absorbance vs time data to the first-order rate equation. Under conditions in which **10a**−**c** are not formed, k_{obs} may appear to decrease because these processes no longer occur in the presence of sufficient concentrations of nucleophile to trap most of the nitrenium ion.

Some of the characteristics of the reactions of **4a** are very different from those previously reported for ester precursors of carbocyclic nitrenium ions. These unusual characteristics include the high proportion of dimeric products (**10a**−**c**) generated, particularly at neutral pH, the significant yield of the reduction product **3a** observed throughout the pH range of the study, and the pH dependence of trapping by N_3^-, Br^-, and d-G. Carbocyclic nitrenium ions generated in aqueous solution usually produce high yields of monomeric products that are generated by attack of H_2O on the nitrenium ion,[6] and very little, if any, reduction product unless the nitrenium ion is a ground-state triplet.[14,17] Dimeric products are rarely observed.[18] Previously reported carbocyclic nitrenium ions do exhibit acid−base properties summarized in eq 3.[6d,19] Because of the magnitude

$$^1ArNH_2^{+2} \underset{+H^+}{\overset{-H^+}{\rightleftharpoons}} {}^1ArNH^+ \underset{+H^+}{\overset{-H^+}{\rightleftharpoons}} {}^1ArN \qquad (3)$$

Ar	pK_a'	pK_a''
Ph		>12
4-biphenylyl	0.1	16
2-fluorenyl	0.6	

of these pK_a values, and the rate constants for trapping by solvent and other nucleophiles, carbocyclic nitrenium ions do not exhibit pH-dependent trapping behavior in the pH range from ca. 2 to 12.

There are only limited product and trapping data available for other heterocyclic nitrenium ions such as **2c**, and the 1-methyl-2-imidazolylnitrenium ion, **20**.[8,20] These species are reported to behave similarly to carbocyclic nitrenium ions.

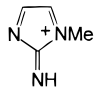

20

The oxidation states and structures of the dimeric products **10a**−**c** are consistent with trapping of the nitrenium ion **5a**, or its conjugate base **7a**, with the amine **3a**. If this is so, the yield of **3a** approaches 50% at neutral pH under our reaction conditions and is approximately 20% at pH < 4.0. These estimates are based on the observed yields of **3a** and 50% of the observed combined yields of **10a**−**c**. Ordinarily, such large yields of the amine reduction product of the nitrenium ion are thought to arise from H$^\bullet$ scavenging by the triplet ion.[14,17] That explanation is inconsistent with the efficient trapping by N_3^-, Br^-, and d-G, which suggests the existence of a reasonably long-lived singlet ion.[6,7,21] If there is an accessible triplet state of **5a** or **7a** (either the ground state or a low lying excited state) addition of H$^\bullet$ donors should increase the yield of **3a** and lead to detectable products arising from reactions of the H$^\bullet$ donor. Falvey and co-workers have successfully employed this strategy to detect the triplet state of *p*-nitrophenylnitrenium ion with the H$^\bullet$ donor Ph_3CH.[14] This hydrocarbon produces a characteristic radical coupling product, **18.** In our solvent system we were limited by the low solubility of Ph_3CH, but saturated solutions of Ph_3CH (2.8×10^{-5} M) produced only marginal changes in the yields of **3a** and other products. The dimer was not detected, but low yields of Ph_3COH, consistent with H^- donation by Ph_3CH, were observed by HPLC. Because of the low solubility of Ph_3CH, it was difficult to make definitive conclusions from these experiments, but they do suggest that the reduction product is not produced from a triplet. The H^- donor **19**[22] had a much larger effect on product yields than did Ph_3CH at similar concentrations, increasing the observed yield of **3a** by 2.6-fold. These data suggest that formation of **3a** is a singlet-state reaction of **5a** and/or **7a**. The source of H^- in the absence of added donors is not known, but could include the products of H_2O

(15) Ingold, C. K. *Structure and Mechanism in Organic Chemistry*, 2nd ed.; Cornell University Press: Ithaca, NY, 1969; pp 418−610.

(16) Richard, J. P.; Jencks, W. P. *J. Am. Chem. Soc.* **1982**, *104*, 4689−4691, 4691−4692; **1984**, *106*, 1383−1396.

(17) Anderson, G. B.; Yang, L. L.-N.; Falvey, D. E. *J. Am. Chem. Soc.* **1993**, *115*, 7254−7262.

(18) One exception occurs during the solvolysis of *N*-acetoxy-2-acetylaminoflourene in aqueous acetone. A product with a structure analogous to that of **10b** is isolated in significant yield: Underwood, G. R.; Kirsch, R. B. *J. Chem. Soc., Chem. Commun.* **1985**, 136−138.

(19) McClelland, R. A.; Kahley, M. J.; Davidse, P. A.; Hadzialic, G. *J. Am. Chem. Soc.* **1996**, *118*, 4793−4803.

(20) Bolton, J. S.; McClelland, R. A. *J. Am. Chem. Soc.* **1989**, *111*, 8172−8181. Gadosy, T. A.; McClelland, R. A. *J. Am. Chem. Soc.* **1999**, *121*, 1, 1459−1465.

(21) McClelland, R. A. *Tetrahedron* **1996**, *20*, 6823−6858.

(22) Zhang, X.-M.; Bruno, J. W.; Enyinnaya, E. *J. Org. Chem.* **1998**, *63*, 4671−4678. Freedman, H. H. In *Carbonium Ions*; Olah, G. A., Schleyer, P. v. R., Eds.; Wiley: New York, 1973; Vol. IV, Chapter 28.

attack on **5a** or **7a**. Both **11** and **12** could serve as reducing agents for **5a** or **7a**.

The equilibrium between **5a** and **7a** may be responsible for the pH dependence of product yields shown in Figure 3. The lack of pH dependence for the products of **4b** observed by HPLC supports this suggestion because **5b** cannot ionize in this manner. If this ionization is responsible for these variations in product yields, **7a** is more susceptible to reduction to **3a** than **5a** is, but both species do apparently produce **3a**. If the dimers **10a**−**c** are produced by trapping of **5a** and **7a** by **3a**, it is clear from the data in Figure 3 that, even at low concentrations ($<1 \times 10^{-5}$ M), **3a** effectively competes with H_2O for both of these species, suggesting that the reaction with H_2O is slow for both **5a** and **7a**. The relatively high kinetic stability of these intermediates toward nucleophilic attack by H_2O is part of the reason that they undergo extensive reduction and dimerization in an aqueous environment. No attempt was made to fit the product yield data to a particular mechanism because of the lack of information concerning individual rate constants, and because the product yields observed under acidic conditions are far from quantitative. The dimeric products **10a**−**c** are structurally analogous to products obtained by the trapping of the *N*-acetyl-*N*-(4-biphenylyl)- and *N*-acetyl-*N*-(2-fluorenyl)nitrenium ions by aniline and *N*,*N*-dimethylaniline in MeOH.[23] Nucleophile/solvent trapping efficiencies were not directly measured but must exceed 500 M^{-1} for both of these ions and both aromatic amines in a solvent that is considerably more nucleophilic than 20 vol % CH_3CN-H_2O.[23] These results show that aromatic amines can be effective traps of nitrenium ions. Dimeric products such as **10a**−**c** are not usually observed because most long-lived nitrenium ions ($1/k_s \geq 10^{-7}$ s) that have been studied in the past do not produce significant amounts of reduction products such as **3a** in the absence of added reducing agents.[6]

The dimerization reaction is reminiscent of a recently discovered dimerization of the α-(*N*,*N*-dimethylthiocarbamoyl)-4-methoxybenzyl carbocation that occurs in 50:50 TFE−H_2O by trapping of the cation with an alkene product formed by an elimination reaction of the cation.[24] The authors concluded that this dimerization could only occur because of the very long lifetime of the cation in this solvent mixture. In the more nucleophilic 50:50 MeOH−H_2O dimerization is suppressed.[24]

The N_3^-, Br^-, and d-G trapping data for **4a** and **4b** provide more definitive evidence for the equilibrium between **5a** and **7a**. In all cases the nucleophilic adduct concentration data fit eq 2 well to produce $(k_{Nu}/k_c)_{obs}$. The rate constant k_c is a combination of terms due to trapping of the nitrenium ion by solvent, k_s, reduction of the nitrenium ion, k_{red}, and dimerization, k_{dim} [**3**] (eq 4). In previous trapping studies of nitrenium ions k_s

$$k_c = k_s + k_{red} + k_{dim}[\mathbf{3}] \tag{4}$$

has been the dominant, if not exclusive, process that occurs in the absence of added nucleophiles.[6,7] That is not entirely the case here. Throughout the pH range of the study **3a** is produced in significant yields, as are **10a**−**c**. The processes that produce these materials are not related to reaction of a nitrenium ion with H_2O, and in the case of the products **10a**−**c**, cannot even be pseudo-first-order in nature. Nonetheless, the product data do fit eq 2 well. Part of the reason for this is that even at low concentrations the nucleophiles do effectively suppress the formation of the dimeric products so that the process measured by k_c when N_3^-, Br^-, or d-G is present is more cleanly pseudo-first-order in nature. Under acidic conditions (pH < 4) the reduction and dimerization processes are suppressed for **4a** (Figure 3) so that $k_s^+ \approx 0.7k_c^+$. Under neutral pH conditions, even if the added nucleophiles suppress the processes leading to **10a**−**c**, a significant part of k_c^0 for **4a** is k_{red}^0, the rate constant for the reduction of **7a**.

If the trapping by each nucleophile is modeled by the mechanism of Scheme 2, the observed trapping ratio $(k_{Nu}/k_c)_{obs}$ is given by eq 5, where all microscopic rate constants are defined

$$(k_{Nu}/k_c)_{obs} = \frac{k_{Nu}^+[H^+] + k_{Nu}^0 K_{a2}}{k_c^+[H^+] + k_c^0 K_{a2}} \tag{5}$$

in Scheme 2. This can readily be rearranged into the form of a titration equation to give eq 6, where $K_{a2}^{app} = k_c^0 K_{a2}/k_c^+$. The

$$(k_{Nu}/k_c)_{obs} = \frac{k_{Nu}^+[H^+]/k_c^+ + k_{Nu}^0 K_{a2}^{app}/k_c^0}{[H^+] + K_{a2}^{app}} \tag{6}$$

logarithmic version of this equation is identical in form to the titration equation that was used to fit the trapping data for **4a** in Figures 5 and 6. The apparent pK_a, pK_{a2}^{app}, is $pK_{a2} + \log(k_c^+/k_c^0)$, and should be invariant to the nucleophile. This expectation is confirmed by the data in Table 3. Since it is likely that $k_c^+ > k_c^0$, it is concluded that $pK_{a2}^{app} > pK_{a2}$.

The mechanism of Scheme 2 requires that replacement of 9-NH by 9-NMe will result in a cation (**5b**) that cannot ionize in the same pH range as **5a** and that will not exhibit pH dependence of $(k_{Nu}/k_c)_{obs}$ in the same pH range. The data in Figures 5 and 6 and Table 3 confirm that trapping of **5b** is independent of pH in this pH range, and, as expected, $(k_{Nu}/k_c)_{obs}$ for **5b** is similar in magnitude to k_{Nu}^+/k_c^+ for **5a**. The somewhat larger value of $(k_{az}/k_c)_{obs}$ for **5b** compared to k_{az}^+/k_c^+ for **5a** is consistent with the expected substituent effect of 9-NMe on k_c if k_{az} for both ions is diffusion-limited and $k_c^+ \approx k_s^+$ for both cations.[6]

Although the experimental results require that both **5a** and **7a** generate the same reaction products with N_3^-, Br^-, and d-G, there is no requirement that the product ratio $[\mathbf{14}]_{max}/[\mathbf{15}]_{max}$ be constant throughout the pH range, and Figure 7 shows that it is not. If all trapping processes are irreversible, the product ratio is equivalent to the ratio of rate constants for trapping of N_3^- at the 3- and 7-positions of **5a** and **7a**: $(k_{3az}/k_{7az})_{obs}$. This ratio, in turn, is given in terms of the microscopic rate constants of Scheme 2 by eq 7, where $k_{az} = k_{7az} + k_{3az}$ for both **5a** and **7a**, and $K_{a3}^{app} = k_{7az}^0 K_{a2}/k_{7az}^+$. Since it is expected that $k_{7az}^+ > k_{7az}^0$, it is also expected that $pK_{a3}^{app} > pK_{a2}$.

$$(k_{3az}/k_{7az})_{obs} = \frac{(k_{3az}^+/k_{7az}^+)[H^+] + (k_{3az}^0/k_{7az}^0)K_{a3}^{app}}{[H^+] + K_{a3}^{app}} \tag{7}$$

The rate constant for N_3^- attack on **5a**, k_{az}^+, is assumed to be diffusion-limited at ca. 5.0×10^9 M^{-1} s^{-1}. Most *N*-arylnitrenium ions with $k_s > 10^4$ s^{-1} have been shown to react with N_3^- under these conditions with a rate constant of ca. 5.0×10^9 M^{-1} s^{-1}.[6] For example, the rate constant for attack of N_3^- on **6** in 5% CH_3CN, $\mu = 0.5$, at 20 °C ($k_s^+ = 3.4 \times 10^4$ s^{-1}) has been directly measured as 4.0×10^9 M^{-1} s^{-1}, while the rate constant for attack of N_3^- on the closely related 2-carbazole nitrenium ion, **21** (eq 8), in 20% CH_3CN, $\mu = 0.1$,

(23) Rangappa, K. S.; Novak, M. *J. Org. Chem.* **1992**, *57*, 1285−1290. Novak, M.; Rangappa, K. S.; Manitsas, R. K. *J. Org. Chem.* **1993**, *58*, 7813−7821.

(24) Williams, K. B.; Richard, J. P. *J. Phys. Org. Chem.* **1998**, *11*, 701−706.

Table 4. Estimated Values for Microscopic Rate Constants and Equilibrium Constants of Scheme 2

constant	estimated value	constant	estimated value
k_{az}^+	5.0×10^9 M^{-1} s^{-1} [a]	k_{3az}^0	1.6×10^6 M^{-1} s^{-1} [e]
k_{3az}^+	3.3×10^9 M^{-1} s^{-1} [b]	k_{7az}^0	4.1×10^5 M^{-1} s^{-1} [e]
k_{7az}^+	1.7×10^9 M^{-1} s^{-1} [b]	k_{Br}^0	1.0×10^4 M^{-1} s^{-1} [d]
k_{Br}^+	1.0×10^8 M^{-1} s^{-1} [c]	k_{d-G}^0	4.1×10^5 M^{-1} s^{-1} [d]
k_{d-G}^+	1.2×10^9 M^{-1} s^{-1} [c]	k_c^0	1.7×10^3 s^{-1} [f]
$k_c^+ \approx k_s^+$	1.4×10^5 s^{-1} [c]	pK_{a2}	3.0[g]
k_{az}^0	2.0×10^6 M^{-1} s^{-1} [d]		

[a] Assumed diffusion-controlled limit. [b] Determined from $[\mathbf{14}]_{max}/[\mathbf{15}]_{max}$ under acidic conditions and estimated k_{az}^+. [c] From k_{Nu}^+/k_c^+ data and estimated k_{az}^+. [d] From k_{Nu}^0/k_c^0 data and estimated k_c^0. [e] Determined from $[\mathbf{14}]_{max}/[\mathbf{15}]_{max}$ under neutral pH conditions and estimated k_{az}^0. [f] Estimated from 2-carbazole nitrenium ion data (ref 25). [g] Average value determined from observed pK_{a2}^{app} and pK_{a3}^{app} of Figures 5−7 and their definitions according to Scheme 2. Standard deviation of the mean ±0.2.

at 20 °C ($k_s^+ = 3.9 \times 10^3$ s^{-1}) has been determined to be 3.9×10^9 M^{-1} s^{-1}.[6d,25]

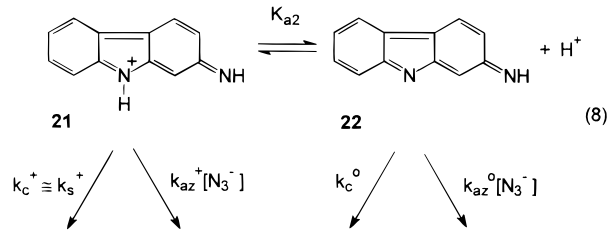

On the basis of this assumption, k_{3az}^+, k_{7az}^+, k_{Br}^+, k_{d-G}^+, and $k_c^+ \approx k_s^+$ were estimated from the rate constant ratios determined under acidic conditions (Table 3) and from $[\mathbf{14}]_{max}/[\mathbf{15}]_{max}$ measured under acidic conditions (Figure 7). These values are gathered in Table 4. Since $k_c^+ \approx k_s^+$ is estimated to be 1.4×10^5 s^{-1}, the assumption that k_{az}^+ is diffusion limited is likely to be valid. The value of k_{d-G}^+ shows that **5a** reacts very efficiently with d-G. Data from the Novak and McClelland laboratories have previously suggested that k_{d-G} reaches a diffusion-controlled limit of ca. 2.0×10^9 M^{-1} s^{-1} for nitrenium ions that have $k_s \geq 10^6$ s^{-1}, so the value for k_{d-G}^+ of 1.2×10^9 M^{-1} s^{-1} for **5a** is quite reasonable.[7] The low yields of **10a−c** observed under acidic conditions are also consistent with the estimated value of $k_c^+ \approx k_s^+$ provided that the trapping of **5a** by **3a** is diffusion limited.

The rate constants for the neutral species **7a** cannot be estimated without additional data. McClelland has directly measured k_c^+ and k_c^0 for the related species **21** and its conjugate base **22** (eq 8) generated from laser flash photolysis of the corresponding 2-azidocarbazole.[25] His results provide k_c^+ of 3.9×10^3 s^{-1} for **21** and k_c^0 of 47 s^{-1} for **22**.[25] If we assume $k_c^+/k_c^0 = 83$ for our system also, the remaining rate constants of Table 4 can be obtained from the rate constant ratios determined under neutral pH conditions (Table 3) and from $[\mathbf{14}]_{max}/[\mathbf{15}]_{max}$ measured under neutral pH conditions (Figure 7). Not surprisingly, **7a** exhibits reduced reactivity toward all the nucleophiles compared to **5a**. In fact, it is somewhat surprising that **7a** does exhibit significant reactivity toward these nucleophiles, and produces the same products with Br$^-$, N$_3^-$, and d-G that **5a** does.

It is unclear from the canonical structure of **7a** (Scheme 2) whether the exocyclic N_2 or the endocyclic N_9 would preferentially serve as the electron sink for attack of nucleophiles on the ring carbons. If N_2 serves in this capacity, one would expect to obtain stable products of nucleophilic attack at C_4, C_6, and C_8, while the expected stable products would occur at C_3, C_5, and C_7 if N_9 serves as the electron sink. The products of attack of Br$^-$ and N$_3^-$ definitely indicate that N_9 is the electron sink for attack of hard nucleophiles on **7a** just as it is for **5a**.

Although **7a** and **5a** generate the same products from reaction with Br$^-$, N$_3^-$, and d-G, reactivity/selectivity considerations based on the Hammond postulate are not likely to apply because of the different charges on the two species and because of the higher propensity of **7a** to undergo reduction and subsequent dimerization.

The measured lower selectivity of **7a** for nonsolvent nucleophiles is, in part, due to the fact that a large proportion of k_c^0 for **7a** does not represent reaction of this species with H_2O. According to our product data (Figure 3) the rate constant for reaction of **7a** with the solvent, k_s^0, may be smaller than 20% of k_c^0, while k_c^+ apparently does predominately represent reaction of **5a** with the solvent. If this is the case, the measured k_{Nu}^0/k_c^0 may underestimate the nucleophile/solvent selectivity of **7a** for purely nucleophilic trapping by at least an order of magnitude. Some support for this proposal comes from the comparison of N$_3^-$/Br$^-$ selectivity of **5a** and **7a** that can be derived from the data of Table 3. For **5a** k_{az}^+/k_{Br}^+ is 49, while k_{az}^0/k_{Br}^0 for **7a** is 210. These results indicate that **7a** is slightly more selective than **5a** in discriminating between these two anionic nucleophiles.

Finally, pK_{a2} can be estimated from pK_{a2}^{app} measured for Br$^-$ and N$_3^-$, and pK_{a3}^{app} measured from the plot of $[\mathbf{14}]_{max}/[\mathbf{15}]_{max}$ (Table 3), and the definitions of the two apparent pK_a values implied in eqs 6 and 7. The three independent data sets provide an average pK_{a2} of 3.0 ± 0.2. The good agreement among the data sets shows that there is good internal consistency in the data, but it does not provide confirmation of the value of pK_{a2} because the three estimates of pK_{a2} would all change by an identical amount if a different k_c^+/k_c^0 were chosen. Nonetheless, the value for pK_{a2} of 3.0 is reasonable in comparison to the pK_{a2} of 5.8 determined for **21**.[25]

Table 5 provides a comparison of arylnitrenium ion selectivities, k_{az}^+/k_s^+ and k_{d-G}^+/k_s^+, for six structurally related carbocyclic and heterocyclic nitrenium ions. This analysis assumes that $k_c^+ \approx k_s^+$ for both **5a** and **5b**. The comparison shows that **5a** and **5b** have selectivities toward N$_3^-$ and d-G that are within a factor of 4 of those exhibited by the *N*-(2-fluorenyl)nitrenium ion, **6**, and have considerably greater selectivity toward those nucleophiles than the *N*-(4-biphenylyl)nitrenium ion, **2d**. Since k_{az}^+ is approximately constant for **2d**, **6**, and **21**,[6d,25] and is likely to be similarly constant for **2a**, **5a**, and **5b**, k_{az}^+/k_s^+ provides a convenient measure of the relative kinetic lability of these ions in an aqueous environment. It is clear that the 2-pyridyl nitrogen of **2a** and **5a** kinetically destabilizes these ions by a factor of ca. 30−300 in comparison to **2d** and **21**, respectively, while

Table 5. Comparison of k_{Az}^+/k_s^+ and k_{d-G}^+/k_s^+ for Several Carbocyclic and Heterocyclic *N*-Arylnitrenium Ions in Aqueous Solution

ion	k_{az}^+/k_s^+ (M^{-1})	k_{d-G}^+/k_s^+ (M^{-1})	ion	k_{az}^+/k_s^+ (M^{-1})	k_{d-G}^+/k_s^+ (M^{-1})
2a	10[a]		**5b**	4.5×10^4 [c]	8.8×10^3 [c]
2d	2.9×10^3 [b]	1.1×10^3 [b]	**6**	1.2×10^5 [d]	2.9×10^4 [d]
5a	3.5×10^4 [c]	8.2×10^3 [c]	**21**	1.0×10^6 [e]	

[a] Source: ref 8. [b] Source: refs 6a,d and 7b,c. [c] Source: this work, it is assumed that $k_c^+ \approx k_s^+$. [d] Source: refs 6d and 7c,d. [e] Source: ref 25.

(25) McClelland, R. A. Personal communication. In view of the results reported here, the McClelland group will reexamine k_c^0 for **22** to determine whether it represents attack of solvent H_2O on **22** or whether it includes reduction and possible dimerization.

the 9-indolyl nitrogen kinetically stabilizes the ion by a factor of ca. 8 compared to the methylene bridge of **6** (compare **6** to **21**). The overall kinetic destabilization of **5a** compared to **6** by a factor of ca. 3.5 is a result of these two opposing effects. The destabilizing effect of the 2-pyridyl nitrogen is apparently inductive in nature, while the stabilizing effect of the 9-indolyl nitrogen is undoubtedly related to the availability of the nonbonded electron pair of that nitrogen for resonance stabilization of the cation.

The deprotonation of **5a** that produces **7a** may be very fortuitous for public health. Experimental data indicate that **3a** is among the most prevalent heterocyclic amines in cooked foods, but its carcinogenic potency measured in animal tests with the purified amines is more than an order of magnitude less than that of the most potent heterocyclic amine carcinogen 2-amino-3-methylimidazo[4,5-f]quinoline (IQ, **23**) and other

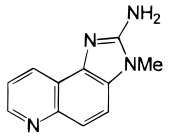

23

heterocyclic amines with structures similar to that of **23**.[1] Literature results suggest that nitrenium ion selectivity may be positively correlated with mutagenicity toward *Salmonella*.[26] To the extent that mutagenicity to *Salmonella* predicts carcinogenicity, **3a** would be expected to be a very potent carcinogen if **5a** were the reactive intermediate present under physiological pH conditions. Since **7a** would be the reactive intermediate responsible for any reactions in vivo, the expected carcinogenic potency of **3a** is a function of the chemistry of **7a**. Our results demonstrate that **7a** reacts with d-G in an aqueous environment ca. 30-fold less efficiently than **5a** does. In an intracellular environment with significantly higher concentrations of reducing agents, that difference would be even more pronounced. The relatively low carcinogenicity of **3a** may be a direct consequence of the chemistry of **7a**.

Experimental Section

General Procedures. The synthesis of 2-amino-9*H*-pyrido[2,3-*b*]-indole (AαC, **3a**) is described in the literature, as is its conversion to the corresponding hydroxylamine.[27,28] C−H connectivity data reported in ^{13}C NMR spectra were obtained from DEPT experiments. ^{13}C NMR spectra for **4a**, **4b**, **10a**−**c**, **11**, and **13**−**16** are provided in the Supporting Information. General methods for purifying solvents, preparing solutions, measuring rate constants by UV methods, and analyzing for products by HPLC have been described elsewhere.[6a,7b,29] Details of the synthesis of 9-methyl-2-nitro-α-carboline, 9-methyl-2-hydroxylamino-α-carboline, 9-methyl-2-amino-α-carboline (**3b**), and 2-amino-3-hydroxy-α-carboline (**11**)[30] are described in the Supporting Information.

Synthesis. 2-*N*-(Pivaloyloxy)-2-amino-α-carboline (4a). A solution of 30 mg (0.151 mmol) of 2-hydroxylamino-α-carboline[28] and 21 μL (0.166 mmol) of *N*-ethylmorpholine in 20 mL of freshly distilled dry benzene was stirred at room temperature for 1 min. Pivaloyl cyanide (18.8 μL, 0.151 mmol) was added to this solution by syringe, and the mixture was stirred for another 15 min. The mixture was washed consecutively with 2 × 5 mL of ice-cold 0.5 M NaOH, 2 × 5 mL of ice-cold 5% $NaHCO_3$, and 2 × 5 mL of ice-cold H_2O. The yellow solution was quickly dried over Na_2SO_4, and after filtration the solvent was removed under vacuum to provide a yellow solid product (29 mg) in 70% yield. This compound is unstable at room temperature but is stable at −40 °C for a period of two weeks. IR (KBr): 3225, 3162, 2973, 1740, 1611, 1587, 1462, 1269 cm^{-1}. ^{1}H NMR (300 MHz, DMSO-d_6): δ 11.52 (1H, s, exchangeable), 10.17 (1H, s, exchangeable), 8.33 (1H, d, J = 8.3 Hz), 7.97 (1H, d, J = 7.6 Hz), 7.40 (1H, d, J = 8.0 Hz), 7.36−7.31 (1H, m), 7.12−7.17 (1H, m), 6.56 (1H, d, J = 8.4 Hz), 1.32 (9H, s). ^{13}C NMR (75.5 MHz DMSO-d_6): δ 176.8 (C), 158.0 (C), 150.7 (C), 138.0 (C), 130.5 (CH), 124.9 (CH), 121.0 (C), 119.8 (CH), 119.4 (CH), 111.0 (CH), 109.6 (C), 99.7 (CH), 38.0 (C), 27.0 (CH_3).

9-Methyl-2-*N*-(pivaloyloxy)-2-amino-α-carboline (4b). This compound was synthesized in 65% yield from the corresponding hydroxylamine on a 15 mg scale by applying the method described above for **4a**. Compound **4b** is unstable at room temperature. A small amount of decomposition was observed over a period of three weeks at −40 °C. ^{1}H NMR (300 MHz, DMSO-d_6): δ 10.32 (1H, s, exchangeable), 8.35 (1H, d, J = 8.3 Hz), 8.01 (1H, d, J = 7.5 Hz), 7.54 (1H, d, J = 8.0 Hz), 7.43−7.35 (1H, m), 7.23−7.18 (1H, m), 6.58 (1H, d, J = 8.3 Hz), 3.78 (3H, s), 1.33 (9H, s). ^{13}C NMR (75.5 MHz, DMSO-d_6): δ 176.8 (C), 157.9 (C), 150.2 (C), 138.9 (C), 130.5 (CH), 124.9 (CH), 120.4 (C), 119.8 (CH), 119.7 (CH), 109.4 (CH), 109.0 (C), 99.6 (CH), 37.9 (C), 27.3 (CH_3), 27.0 (CH_3).

Kinetics and Product Studies. All reactions were performed in 20 vol % CH_3CN-H_2O, μ = 0.5 ($NaClO_4$), at 20 °C. Buffers used to maintain pH were 0.02 M tris/trisH^+, Na_2HPO_4/NaH_2PO_4, NaOAc/AcOH, and $NaHCO_2/HCO_2H$ at pH > 2.5 and $HClO_4$ solutions at pH ≤ 2.5. NaBr and 2′-deoxyguanosine (d-G) solutions were made at high concentrations (0.45 M for NaBr, 30 mM for d-G), μ = 0.5, and the appropriate pH, and diluted into the working range with buffers of the same pH containing no nucleophile. A similar procedure was followed for NaN_3 in phosphate buffers of pH ≥ 6.0. For N_3^- solutions prepared at pH 3.7−5.7, 0.02 M N_3^-/HN_3 buffers of the appropriate pH and ionic strength were prepared and diluted into the working range with 0.02 M NaOAc/HOAc buffers of identical pH.

Stock solutions of both **4a** and **4b** were made in DMF at concentrations of ca. 2.0 × 10^{-3} M. Injection of 15 μL of these stock solutions into 3.0 mL of buffer generated reaction solutions of initial concentrations of ca. 1.0 × 10^{-5} M in **4a** or **4b**. Wavelengths monitored for kinetics studies for **4a** were 360 nm at pH ≥ 1.7 and 320 nm for pH < 1.7. For **4b**, kinetics studies were performed at 310 nm. Initial absorbance measurements for both compounds for the spectrophotometric titration were made at 360 nm. Absorbance vs time data were fit to a standard first-order rate equation to provide k_{obs}.

Reaction products were monitored by HPLC with UV detection at 340 nm for **4a** and 330 nm for **4b**. HPLC conditions were C-8 analytical reversed-phase column, 75:25 MeOH/H_2O eluent buffered with 0.05 M 1:1 NaOAc/AcOH, at a flow rate of 1.0 mL/min. The same concentrations of **4a** and **4b** utilized in the kinetic studies were employed in the product analyses. N_3^-, Br^-, and d-G concentrations were kept in at least 5-fold excesses over **4a** and **4b**.

Major decomposition products of **4a** in Br^- (**13**), N_3^- (**14**, **15**), and d-G (**16**) solutions were isolated and purified from large-scale decomposition reactions in buffered aqueous solution. A solution of 2.0 × 10^{-2} M **4a** was prepared in 10 mL of dry DMF. This solution was added to 500 mL of NaN_3 solution (pH 6.32, 0.47 M NaN_3) or NaBr solution (pH 4.92, 0.48 M NaBr) or 100 mL of d-G solution (pH 7.35, 0.03 M d-G), at 20 °C in 1 mL aliquots at 7 min intervals. Reactions were allowed to continue for 30 min after the last addition. The products **13**, **14**, and **15** were isolated by extraction with EtOAc (3 × 50 mL). After solvent evaporation, products were purified as

(26) Ford, G. P.; Griffin, G. R. *Chem.-Biol. Interact.* **1992**, *81*, 19−23. Novak, M.; VandeWater, A. J.; Brown, A. J.; Sanzenbacher, S. A.; Hunt, L. A.; Kolb, B. A.; Brooks, M. E. *J. Org. Chem.* **1999**, *64*, 6023−6031.
(27) Hibino, S.; Sugino, E.; Kuwada, T.; Ogura, N.; Shintani, Y.; Satoh, K. *Chem. Pharm. Bull.* **1991**, *39*, 79−80.
(28) Kazerani, S.; Novak, M. *J. Org. Chem.* **1998**, *63*, 895−897.
(29) Novak, M.; Kahley, M. J.; Lin, J.; Kennedy, S. A.; James, T. G. *J. Org. Chem.* **1995**, *60*, 8294−8304. Novak, M.; Brodeur, B. A. *J. Org. Chem.* **1984**, *49*, 1142−1144. Novak, M.; Pelecanou, M.; Roy, A. K.; Andronico, A. F.; Plourde, F. M.; Olefirowicz, T. M.; Curtin, T. J. *J. Am. Chem. Soc.* **1984**, *106*, 5623−5631.
(30) Raza, H.; King, R. S.; Squires, R. B.; Guengerich, F. P.; Miller, D. W.; Freeman, J. P.; Lang, N. P.; Kadlubar, F. F. *Drug Metab. Dispos.* **1996**, *24*, 385−400.

follows. The bromide product **13** was purified by column chromatography on silica gel (eluent 70:30 CH_2Cl_2/EtOAc). The azide adducts **14** and **15** were purified by C_{18} reversed-phase column chromatography using 60:40 MeOH/H_2O as eluent. In the case of **16**, water was removed from the aqueous d-G buffer solution by freeze-drying. The remaining residue was washed with 4 × 10 mL of EtOAc to isolate **16**. The EtOAc was evaporated to dryness, and the residue containing **16** was purified by C_{18} reversed-phase column chromatography using 30:70 to 55:45 MeOH/H_2O as eluent.

Decomposition products of **4a** in buffered aqueous solution were isolated from reactions run at an initial concentration of ca. 3×10^{-4} M **4a**. A solution of 2×10^{-2} M **4a** was prepared in 15 mL of dry DMF. This solution was added to 1 L of phosphate buffer (pH 6.8) at 20 °C in 1 mL aliquots at 7 min intervals. Reactions were allowed to continue for 3 h after the last addition of **4a**. A precipitate that formed during the reaction was removed by filtration from the solution. Among other minor products, **10b** and **10c** were isolated and purified from this precipitate by C_{18} reversed-phase column chromatography (eluent 30:70 to 70:30 MeOH/H_2O). After removal of the precipitate, the aqueous solution was extracted with 3 × 50 mL of EtOAc. The organic layers were combined and dried over Na_2SO_4. The Na_2SO_4 was filtered and the EtOAc was removed by rotary evaporation, resulting in a residue containing a mixture of **3a** and **10a** among other minor products. Separation and purification were performed by C_{18} reversed-phase column chromatography (eluent 30:70 to 70:30 MeOH/H_2O). Detailed IR, NMR, and MS characterization of **10a**−**c** and **13**−**16** is provided in the Supporting Information.

Acknowledgment. This work was supported by a grant from the American Cancer Society (CN-172). NMR spectra were obtained on equipment originally made available through an NSF grant (CHE-9012532) and subsequently upgraded through an Ohio Board of Regents Investment Fund grant. Electron ionization high-resolution mass spectra were obtained at the Ohio State University Chemical Instrumentation Center, and MALDI-TOF mass spectra were obtained at Miami on equipment funded by the NSF-ARI program (Grant CHE-9413529) and the Ohio Board of Regents Action Fund. We thank Dr. Robert A. McClelland for sharing preliminary data with us and for helpful discussions.

Supporting Information Available: Tables of rate constants for the decomposition of **4a** and **4b**, tables of Br^-, N_3^- and d-G trapping results for **4a** and **4b**, synthesis of **3b** and **11**, characterization of **10a**−**c** and **13**−**16**, and ^{13}C NMR spectra for **4a**, **4b**, **10a**−**c**, **11**, and **13**−**16** (PDF). This material is available free of charge via the Internet at http://pubs.acs.org.

JA993433E